

Deriving ACR shock spectrum from observations of the energetic neutral atoms

A. Czechowski¹, M. Hilchenbach², and K.C. Hsieh³

¹Space Research Centre, Polish Academy of Sciences, Bartycka 18A, PL-00 716 Warsaw, Poland

²Max-Planck-Institut für Aeronomie, Max-Planck-Strasse 2, D-37191 Katlenburg-Lindau, Germany

³Physics Department, University of Arizona, Tucson AZ 85721, U.S.A.

Abstract. One of the sources of the energetic neutral atoms (ENA) in the heliosphere are the low-energy (up to few 10^2 keV) anomalous cosmic ray (ACR) ions in the outer heliosphere, close to and beyond the solar wind termination shock. The ENAs can penetrate into the inner solar system, and, if observed, provide the information about the ACR distribution in the source region. Using the results of numerical simulations of the ACR spatial and energy distributions in the heliosphere, we derive approximate relations between the ENA energy spectrum as observed at the orbit of the Earth and the ACR spectrum near the solar wind termination shock. With some assumptions about the parameters of the heliosphere, these relations allow one to obtain the ACR shock spectrum from the observed ENA spectrum. We apply this method to the data from CELIAS/HSTOF and discuss the results for the ACR spectrum.

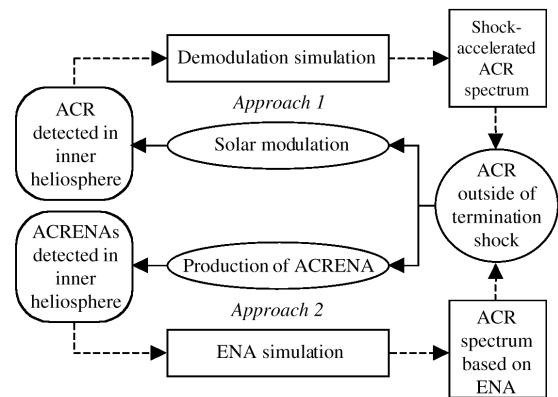


Fig. 1. Two approaches to the study of ACR.

1 Introduction

The anomalous cosmic ray (ACR) particle spectrum in the outer heliosphere may be indirectly observed by means of the energetic neutral atoms (ENA) into which the ACR particles convert when neutralized by charge-exchange with the atoms of the background gas (Hsieh et al. 1992; Grzedzielski 1993; Czechowski et al. 1995, 2001). As the ENA flux is given by the integral along the line-of-sight, the information about the ACR spectrum obtained in this way is an average over the region of the source (the outer heliosphere) and some information about the heliospheric structure is needed for its interpretation.

In this paper we consider the question of how the ACR spectrum at the termination shock can be derived from the observations of the ENA (Approach 2 in Figure 1). We find that for the low energy region (suggested to be 10-50 keV by the model simulations), where the ACR distribution in the heliotail is determined by convection and charge-exchange

loss term while the effects due to spatial diffusion can be disregarded, the ACR shock spectrum can be derived from the ENA flux from the heliotail direction without any additional information about the heliosphere. In the case when the heliopause is not too distant and can be considered to be approximately a free escape boundary, it is possible to obtain the shape of the ACR shock spectrum from the ENA flux from the apex direction, assuming only that the average density ratio of neutral He and H in the region between the termination shock and the heliopause is known. The interpretation of the ENA flux from the heliotail (unless the energy is low enough to neglect ACR diffusion) requires additional information ($\Lambda(E)$, the distance scale of the ACR distribution as a function of energy).

We apply our results to the CELIAS/HSTOF ENA hydrogen data (Hilchenbach et al. 1998, 2000). Unfortunately, the energy region covered by the observations is too narrow to make a meaningful estimation of the slope of the spectrum.

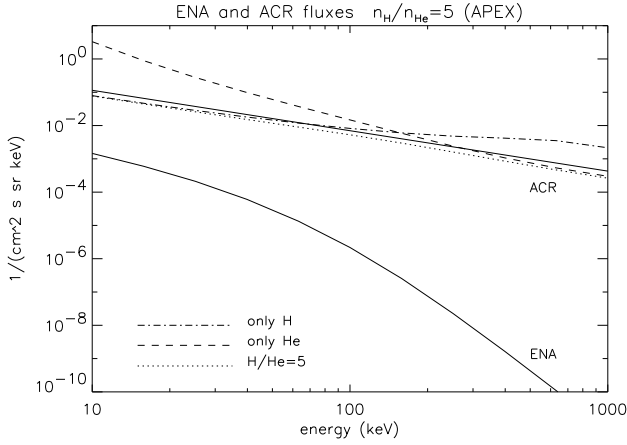


Fig. 2. The ACR proton spectrum at the shock and the calculated ENA H spectrum from the LISM apex direction from the simulation using Kausch's model (solid lines). The dashed lines show the estimations of the ACR spectrum at the shock obtained from the calculated ENA spectrum by means of Eqs. (2, 3) assuming $\Lambda = 30$ AU. The neutral gas densities between the termination shock and the heliopause are taken respectively as $(n_{\text{H}} = 0.05 \text{ cm}^{-3}, n_{\text{He}} = 0)$, $(n_{\text{H}} = 0, n_{\text{He}} = 0.01 \text{ cm}^{-3})$, $(n_{\text{H}} = 0.05 \text{ cm}^{-3}, n_{\text{He}} = 0.01 \text{ cm}^{-3})$

2 The ENA flux and the ACR shock spectrum

The relation between the ACR flux J_{ACR} beyond the termination shock and the ENA flux J_{ENA} observed at the orbit of the Earth is given by the integral along the line of sight

$$J_{ENA}(E, \mathbf{n}) = \int_0^{\infty} dr J_{ACR}(E, r, \mathbf{n}) (\sigma_{\text{cx,H}} n_{\text{H}} + \sigma_{\text{cx,He}} n_{\text{He}}) \quad (1)$$

where E is the particle energy, r is the distance along the line of sight and \mathbf{n} the direction of the flux (the extinction factor is negligible). We consider the relatively low energy region (up to $\sim 10^2$ keV) where the charge exchange cross sections $\sigma_{\text{cx,H}}, \sigma_{\text{cx,He}}$ are not too small. Because the low energy ACR flux is strongly suppressed upstream of the shock, only the region downstream will contribute to the integral. Assume that the ACR flux falls with the distance downstream from the shock as

$$J_{ACR}(r) = J_{ACR}|_{\text{shock}} \exp(-r/\Lambda) \quad (2)$$

The distance scale of the falloff Λ depends in general on the energy and on the direction. Substituting into Eq. (1):

$$J_{ENA} = \Lambda (\sigma_{\text{cx,H}} n_{\text{H}} + \sigma_{\text{cx,He}} n_{\text{He}}) J_{ACR} \quad (3)$$

The model simulations of the ACR distribution show that in the apex direction the value of Λ is almost independent of the ACR energy (Fig. 12 of Czechowski et al. 2001). This conclusion is based on the models for which the diffusion coefficient outside the heliopause is taken to be much larger than inside: the ACR distribution must then fall to a low value at the heliopause, which is almost a free escape boundary. The scale Λ is then of the order of the distance from the shock

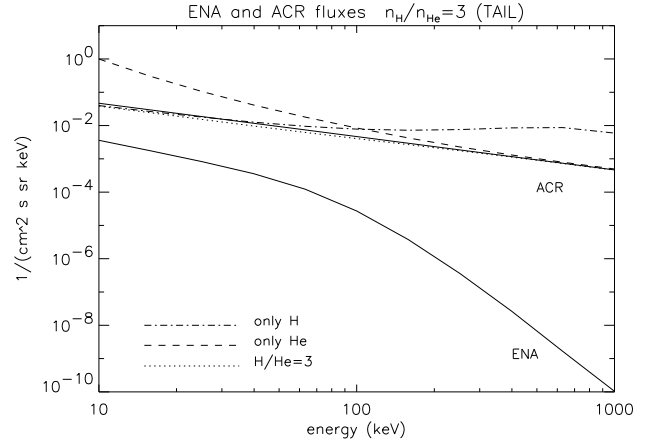


Fig. 3. As Fig. 2, but for the ENA flux from the anti-apex direction. at the shock obtained from the ENA spectrum by means of Eq. (1) is used with $\Lambda(E)$ derived from Kausch's model. The neutral densities are $(n_{\text{H}} = 0.03 \text{ cm}^{-3}, n_{\text{He}} = 0)$, $(n_{\text{H}} = 0, n_{\text{He}} = 0.01 \text{ cm}^{-3})$, $(n_{\text{H}} = 0.03 \text{ cm}^{-3}, n_{\text{He}} = 0.01 \text{ cm}^{-3})$

to the heliopause in the apex direction (about 30 AU in most models).

This suggests that if the ACR ENA energy spectrum from the apex direction is known, the corresponding ACR energy spectrum can be deduced up to an approximately constant (energy-independent) factor:

$$J_{ACR}|_{\text{apex}} \propto \frac{J_{ENA}|_{\text{apex}}}{\sigma_{\text{cx,H}} n_{\text{H}} + \sigma_{\text{cx,He}} n_{\text{He}}} \quad (4)$$

The information needed to derive the shape of the ACR energy spectrum is then reduced to the knowledge of the average H/He density ratio along the line of sight, between the shock and the heliopause.

In the anti-apex direction one needs to know also the energy dependence of Λ . In the low energy region, where the spatial diffusion of the ions is negligible compared to convection and loss rate due to charge-exchange it is possible to deduce the energy dependence of Λ from the transport equation, provided that the plasma flow beyond the shock can be taken to be approximately incompressible. In this case one can neglect diffusion and adiabatic acceleration terms in the transport equation and obtain for Λ

$$\Lambda = \frac{V}{u (\sigma_{\text{cx,H}} n_{\text{H}} + \sigma_{\text{cx,He}} n_{\text{He}})} \quad (5)$$

where V is the plasma speed downstream of the shock and u the speed of the ACR particle. Including diffusion would decrease the value of Λ while the effect of plasma flow compressibility depends on the sign of the divergence ($\nabla \cdot \mathbf{V}$).

With this approximation used, the ACR spectrum in the anti-apex direction is given by

$$J_{ACR}|_{\text{antiapex}} = \frac{u}{V} J_{ENA}|_{\text{antiapex}} \propto E^{1/2} J_{ENA}|_{\text{antiapex}} \quad (6)$$

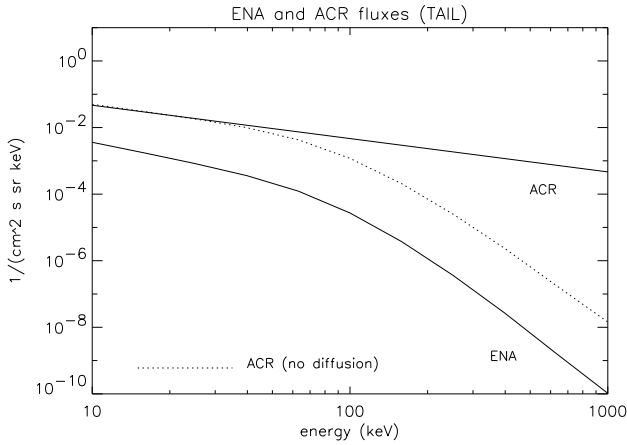


Fig. 4. The ACR proton spectrum at the shock and the calculated ENA H spectrum from the anti-apex direction from the simulation using Kausch's model (solid lines). The dashed line shows the estimation of the ACR spectrum at the shock obtained from the ENA spectrum by means of Eq. (5) assuming $V = 100$ km/s.

where E is the particle energy. This approximation should be applicable in the low energy region, assuming that the adiabatic acceleration effects due to plasma flow divergence term are not too strong. We found that the region of applicability of Eq. (6) has also a low energy limit (1-few keV), where large spatial gradients in the distribution of ACR make diffusion effects become important.

The expressions for the ACR flux in terms of the ENA spectrum given by the Eqs. (3), (4) and (6) are approximate (in particular, the modulation of the ACR spectrum due to nonzero divergence of the plasma flow is not taken into account). In order to estimate the validity of these approximations we have used the results for the ENA flux calculated in a model (Czechowski et al. 2001) to derive the approximate ACR spectrum at the shock. This spectrum was then compared with the ACR spectrum which was used in the model calculation. The results are presented in Figures 2 to 4 and the agreement is good for this particular case. One must, however, keep in mind that the present models of the ACR distribution beyond the termination shock are still rather simplified (for example, the spatial diffusion is assumed to be isotropic) which may restrict the validity of the conclusions.

3 CELIAS/HSTOF ENA observations and the ACR flux

The first detection of what may be the ENA of heliospheric origin (Hilchenbach et al. 1998) is due to CELIAS/HSTOF, operating on board of the SOHO spacecraft, situated near the Lagrangian point L1 between Earth and the Sun. The data which can be used to estimate the spectrum consist of the three low energy data points (the higher energy data contain presumably a large fraction of the charged flux) covering the energy range of 58-88 keV. We include the changes due to in-flight new calibration of the instrument (Hilchenbach et al.

2000) which raised the previous estimations of the flux by a factor of 10. We consider the flux from the forward direction (LISM apex region) and from the anti-apex direction which should be close to that of the heliotail. The characteristic signature of the ENA of ACR origin is that the maximum flux should arrive from the LISM anti-apex (heliotail) direction. The model simulations (Czechowski et al. 2001) based on a particular gas-dynamical solution for the heliosphere (Fahr et al. 2000) imply, however, a larger anti-apex to apex flux ratio than observed in the data. One possible explanation is that a fraction of the observed flux is not due to ACR (Hsieh et al. 1999; Kota et al. 2001). Another possibility, which we assume, is that the model of the heliosphere used in the ACR ENA calculations should be modified to increase the ENA flux from the apex direction.

Figure 5 shows the results of the χ^2 fits to the data assuming that the ACR flux at the shock is given by a simple power law $E^{-\gamma}$. Note that in fitting the apex ENA data we have assumed the size of the forward heliosphere and the average n_H there to be larger than in the model of the heliosphere based on Kausch's solution.

4 Discussion

The model simulations of the ACR distribution beyond the termination shock and of the ENA flux from this source suggest that the observations of ENA may in some cases be used to obtain information about the ACR spectrum at the termination shock without detailed knowledge of the heliospheric parameters. Of particular interest is the low energy region (10-50 keV, although this is a model dependent estimation) for which the relation between the ACR spectrum and the ENA flux from the heliotail simplifies because the ACR spatial distribution is then determined by the same charge exchange processes which produce the ENA. This energy region is within the range of the IMAGE/HENA (Roelof, 2000) and Cassini/INCA, so that the measurements of the heliospheric ENA by these instruments would be of high interest.

The CELIAS/HSTOF observations of the ENA flux are unfortunately too restricted in energy (58-88 keV) to determine the source spectrum. The reasonable values of the slope parameter ($\gamma = 1 - 1.5$) are not excluded by the data. The ACR flux intensity at the shock implied by the ENA data is high (the results of Stone et al. 1996, when extrapolated to low energy, imply the flux of $7 \cdot 10^{-3} (cm^2 s sr keV)^{-1}$ at 100 keV) in particular in the region close to the LISM apex. This may indicate that at least a fraction of the observed ENA is not due to ACR (high ≤ 100 keV proton flux at the shock can be obtained from the models using pick-up ion pre-acceleration: Czechowski et al. 1999; Fahr and Lay, 2000). Alternatively, the model of the heliosphere must be modified (larger size and higher value of the neutral H density) to enhance the production of the ENA from the forward region.

Acknowledgements. A.C. wishes to thank the Max-Planck-Institut für Aeronomie for hospitality.

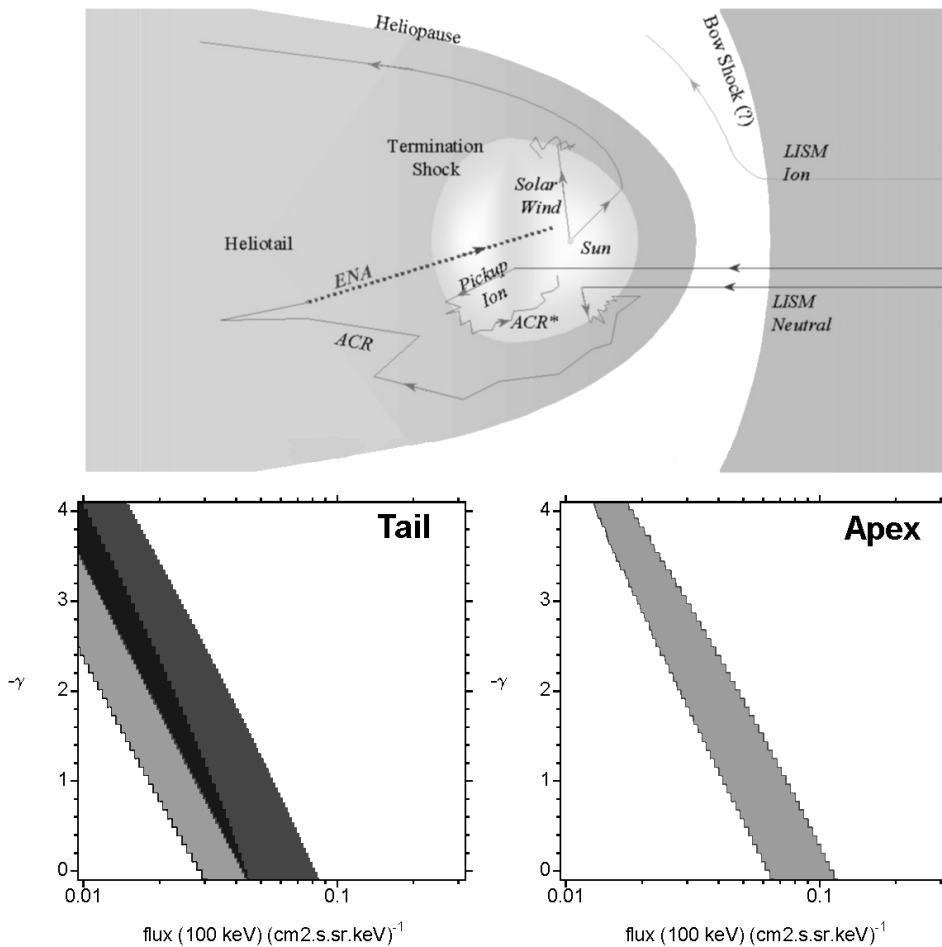


Fig. 5. The upper panel is the schematic view of the heliosphere with a typical history of an ACR ENA particle. The lower panels show the results of the χ^2 fits to the ENA data assuming that the ACR flux at the shock is given by a simple power law $E^{-\gamma}$ (position-dependent). The x axis shows the ACR flux intensity value at 100 keV ($J(100)$). The regions of $\chi^2 \leq 3$ are shown. The best fits (with χ^2 of the order of 1 % or less) are listed below. For the tail direction we show two overlapping regions, the leftmost obtained using Eq. (6) (best fit $\gamma = 3.92$, $J(100) = 7.7 \cdot 10^{-3}$) and the other using $\Lambda(E)$ from the model simulation based on Kausch's solution (best fit $\gamma = 2.01$, $J(100) = 2.7 \cdot 10^{-2}$). The plot in the righthand panel is derived from the apex ENA using Eq. (3) and assuming $\Lambda=45$ AU, $n_{\text{H}}=0.15 \text{ cm}^{-3}$, $n_{\text{He}}=0.01 \text{ cm}^{-3}$ for the forward heliosphere (best fit $\gamma=0.2$, $J(100) = 7.9 \cdot 10^{-2}$). If the model of the heliosphere based on Kausch's solution (with $\Lambda=30$ AU and $n_{\text{H}}=0.05 \text{ cm}^{-3}$) would be used for the forward region, the result for the ACR flux would be unrealistically high (best fit $\gamma=0.39$, $J(100) = 0.27$).

References

- Czechowski, A., H.J. Fahr, H. Fichtner, and T. Kausch, Salt Lake City, Utah, August 17-25 1999, Eds. D. Kieda, M. Salamon & B. Dingus, Vol.7, p. 464, 1999.
- Czechowski, A., H. Fichtner, S. Grzedzielski, M. Hilchenbach, K.C. Hsieh, J.R. Jokipii, T. Kausch, J. Kota, and A. Shaw, *A&A*, **368**, 622, 2001.
- Czechowski, A., S. Grzedzielski, and I. Mostafa, *A&A*, **297**, 892, 1995.
- Fahr, H.J., T. Kausch, and H. Scherer, *A&A*, **357**, 268, 2000.
- Fahr, H.J., and G. Lay, *A&A*, **356**, 327, 2000.
- Grzedzielski, S., *Adv. Space Res.*, **13**, (6)147, 1993.
- Hilchenbach, M., K.C. Hsieh, D. Hovestadt, B. Klecker, H. Grünwaldt et al., *ApJ*, **503**, 916, 1998.
- Hilchenbach, M., K.C. Hsieh, D. Hovestadt, R. Kallenbach, A. Czechowski, E. Möbius, and P. Bochsler, presented at the COSPAR Colloquium The Outer Heliosphere: The New Frontiers, Potsdam 24-28 July 2000.
- Hsieh, K.C., A. Czechowski, J. Kota, J.R. Jokipii, and M. Hilchenbach, Proceedings of the 26th International Cosmic Ray Conference, Salt Lake City, Utah, August 17-25 1999, Vol.6, p. 492, 1999.
- Hsieh, K.C., K.L. Shih, J.R. Jokipii, and S. Grzedzielski, *ApJ*, **393**, 756, 1992.
- Kota, J., K.C. Hsieh, A. Czechowski, J.R. Jokipii, and M. Hilchenbach, *J. Geophys. Res.*, (in press), 2001.
- Roelof, E.C., presented at the COSPAR Colloquium The Outer Heliosphere: The New Frontiers, Potsdam 24-28 July 2000.
- Stone, E.C., A.C. Cummings, and W.R. Webber, *J. Geophys. Res.*, **101**, 11017, 1996.